http://dx.doi.org/10.5012/bkcs.2014.35.5.1305

The Enhanced Physico-Chemical and Electrochemical Properties for Surface Modified NiO Cathode for Molten Carbonate Fuel Cells (MCFCs)

Hee Seon Choi, Keon Kim,* and Cheol-Woo Yi†,*

*Department of Chemistry, Korea University, Seoul 136-701, Korea. *E-mail: kkim@korea.ac.kr*
†Department of Chemistry and Institute of Basic Science, Sungshin Women's University, Seoul 142-732, Korea
**E-mail: cheolwoo@sungshin.ac.kr*
Received November 6, 2013, Accepted January 3, 2014

The nickel oxide, the most widely used cathode material for the molten carbonate fuel cell (MCFC), has several disadvantages including NiO dissolution, poor mechanical strength, and corrosion phenomena during MCFC operation. The surface modification of NiO with lanthanum maintains the advantages, such as performance and stability, and suppresses the disadvantages of NiO cathode because the modification results in the formation of $LaNiO_3$ phase which has high conductivity, stability, and catalytic activity. As a result, La-modified NiO cathode shows low NiO dissolution, high degree of lithiation, and mechanical strength, and high cell performance and catalytic activity in comparison with the pristine NiO. These enhanced physico-chemical and electrochemical properties and the durability in marine environment allow MCFC to marine application as a auxiliary propulsion system.

Key Words : Molten carbonate fuel cell (MCFC), Surface modification, Lanthanum oxide (La_2O_3), Lanthanum nickel oxide ($LaNiO_3$), Nickel oxide (NiO) cathode

Introduction

Molten carbonate fuel cell (MCFC) has great advantages such as the operation without expensive platinum-based catalysts, the use of variety of fuel gases including natural gas, carbon monoxide and hydrogen, and the utilization of the high-temperature waste heat because it enables the catalytic reaction at high operating temperature, 650 °C.[1] Due to these advantages, MCFC has been widely employed in the field of stationary power generation system. Moreover, recently, many international conventions have regulated and controlled the emission of greenhouse gas and environmental pollutants in the field of maritime and it is an urgent situation.[2] The technology development for pollutant reduction proposes to use the high efficient power generator instead of ordinary internal combustion engine (especially diesel engine)[3] to reduce the emission of pollutant such as NO_x, SO_x, VOC, PM, *etc*. Thus, the marine industry is developing marine application for fuel cell system as auxiliary power units because fuel cell does not incurs pollutants and provides very high overall efficiency.[2,4,5] However, there are some disadvantages of MCFC including cathode dissolution phenomena, creep at anode and current collector, and corrosion of separator. As a result, cell performance is reduced during MCFC operation and they suppress the long-term operation of MCFC.[1] Particularly, the dissolution of cathode leads to the formation of Ni^{2+} ions diffusing toward the anode. Subsequently, the dissolved Ni^{2+} ions are reduced and precipitated in the matrix where it encounters H_2 diffused from the anode, and the precipitate causes an internal short-circuit of MCFC. Theses structural changes of the cathode caused by the reduction give challenges.[6-8]

Two types of dissolution mechanism of NiO (acidic or basic dissolution) have been proposed and it is reported that the solubility of NiO depends on the acid-base properties of the molten carbonate or carbonate mixture.[9] In order to solve the problem of NiO dissolution, many investigators have studied alternative electrolytes and cathodes. From results of the NiO dissolution as a function of the composition of electrolytes (Li_2CO_3/K_2CO_3), it is found that the solubility is decreased with an increase in the concentration of Li_2CO_3 in the electrolyte.[10] Moreover, the addition of alkaline earth metal oxide, alkaline earth metal carbonates, rare earth metal oxide, and/or rare earth metal carbonates increase the basicity of the molten carbonate electrolyte,[11,12] and simultaneously Ni dissolution decreases.[13-21] Another possible way to suppress the Ni dissolution, coating or surface modification of NiO cathode with a conducting and stable materials such as Co/Mg, Co/Ce, $LiCoO_2$, TiO_2, ZnO, La_2O_3 and $MgFe_2O_4$-coated NiO cathode.[22-30] In addition, La-substituted materials, $LaCoO_3$, $LaNiO_3$, $La_{0.8}Sr_{0.2}CoO_3$, and $La_{0.8}Sr_{0.2}MnO_3$ including perovskite type oxides have a great attention because of high conductivity, heat resistance and stability of the complex oxides.[31-37] Despite many studies related to La species for MCFC application, most of them are focused to the use of lanthanum species as an additive in molten carbonate electrolyte[11,12,14,16,17,19-21,38] to decrease the dissolution of NiO by increasing the basicity of the electrolyte or perovskite oxide ($La_{1-x}A_xBO_3$) electrodes itself.[31-37] Only a few studies[22,23] have been done with La-modified Ni electrode, but they just made a pellet and measured the solubility of Ni and/or impedance spectra. In the present study, we have prepared alternative NiO cathodes as Ni powders modified with lanthanum by Pechini method and investigated minor phase

and phase transformation of La-modified Ni cathodes and unit cell operation for the first time. The modified cathode improves its stability ascribed to the formation of a stable phase on the surface of NiO. The La-impregnated NiO cathode has been shown to the lower resistance to charger-transfer processes than pure Ni cathode[37] since lanthanum oxide has high catalytic activity for oxygen reduction reaction (ORR).[26,39] We have mainly focused on La-modified NiO cathode and investigated cell performance, Ni dissolution, lithiation, etc. For marine application, mechanical strength of cathodes and the effect of NaCl on the cathode have also been investigated.

Experimental

Preparation of La-modified Ni Powders and the Modified Cathodes. The La-modified Ni powder as a cathode material for MCFC was prepared by Pechini method. As a source of lanthanum, La(III) nitrate hexahydrate ($La(NO_3)_3 \cdot 6H_2O$) was dissolved in distilled water, and then citric acid and ethylene glycol as chelating agents were added into the lanthanum nitrate solution. By adding ammonia water, the pH of the solution increases to 8–9, and then the Ni powder (particle size = 2–3 μm, Inco nickel 255) was added into the solution. The resulting solution was heated with stirring at 80 °C until the solvent was evaporated. The obtained gel precursor was calcined at 500 °C for 3 h to remove organic components and all decomposable materials. The calcination temperature was determined through thermo-gravimetric analysis (TGA) under air condition.

The cathode was prepared through tape casting method, and the slurry consists of binder (polyvinyl butyral, Monsanto), plasticizer (dibutyl phthalate, Junsei), dispersant (BYK110, Disper), defoamer (D354, Dappo), and solvent (ethanol : toluene = 70 : 30 wt %, Junsei). The mixture of La-modified Ni powder and slurry was ball-milled for 5 hours, and it is subsequently degassed in a vacuum oven for 20 minutes. The green sheet (thickness = 0.7–0.8 mm) was obtained by a double doctor blade, and then it was allowed to be dried for 24 h at room temperature. The dried green sheet was sintered at 750–950 °C under the reducing atmosphere (Ar : H_2= 70 : 30%).

Characterization of Modified Powder and Cathode. TGA of the gel precursors was performed to characterize the thermal behavior of the samples and to optimize the calcination temperature for the gel precursor. The microstructures of cathode and powder were observed by field emission-scanning electron microscopy (FE-SEM, Hitachi S-4300) at an acceleration voltage of 25 kV. The distributions of nickel and lanthanum were observed by energy dispersive spectroscopy (EDS, Horiba EX-200). The composition and phase of the prepared powders were analyzed by X-ray diffraction (XRD) using a Bruker D8 Focus equipped with a Cu target. The XRD data were obtained at a scan rate of 0.2 sec/step in the 2θ range of 10–90°. The pore properties of sintered electrode were investigated using Archimedes method.

In order to minimize cracking of the cathode due to the vibration and inclination in the marine environment, the cathode should have adequate mechanical strength. The mechanical strength of cathode was examined by three point bending strength measurements (QC-508E, Cometech Co.). Moreover, the morphology and chemical change of cathode at marine atmospheric environment were investigated by SEM, XRD, infrared spectroscopy (IR) and Raman spectroscopy with the pristine and La-modified cathode immersed into 10 wt % NaCl solution at 80 °C.

The solubility test[40] for pristine and La-modified NiO cathodes is carried out in order to investigate the Ni dissolution. The solubility test of cathode materials is performed for 300 h after CO_2 was blown at 500 °C for 24 h. About 1.5 g of pristine NiO cathode or modified NiO cathode was added into 100 g of molten carbonates and ~0.3 g of sample was periodically collected using alumina pipette. Each carbonate sample was transferred to a clean alumina crucible, and the solidified carbonates are dissolved in 1.0 M HNO_3 aqueous solution. Subsequently, it is diluted with 20 mL of distilled water after solvent is evaporated. Concentration of Ni was measured with inductively coupled plasma atomic emission spectroscopy (ICP-AES, Elan DRC II/Perkin Elmer).

Performance of Unit Cell. The detailed experimental procedure and cell assembly are described elsewhere.[28,40] The unit cell test was performed for 300 h with 3 × 3 cm^2 electrode at 650 °C to investigate the cell performance and electrochemical properties. The open-circuit voltage and the closed-circuit voltage were measured at the current density of 150 mA/cm^2. Except for the cathode, other components were commercial products. The porous Ni-10 wt % Al plaque (Twin Energy , Korea) was used as a standard anode material and the Li/K carbonate sheet (62/38 mol %; Twin Energy, Korea), porous γ-$LiAlO_2$ (Twin Energy, Korea) sheet, SUS 316 and Ni are used as electrolyte, matrix and current collector, respectively. The anode gas is a mixture of H_2/CO_2 (66.7 : 33.3%) humidified at 50 °C and the cathode gas is a mixture of Air : CO_2 (70 : 30%).

Results and Discussion

The Modified Powders. In order to investigate the thermal behavior of the gel precursor, TGA was measured and the results of TGA are shown in Figure 1. The weight loss of the gel precursors is completed at ~500 °C and three discrete weight loss regions are observed at 100–200, 200–350, and 350–500 °C. The first weight loss region is mainly attributed to the removal of excess ethylene glycol and residual water and dehydration of citric acid. The second region is the decomposition of citric acid and the partial decomposition nitrate species. As a result, lanthanum oxynitrate species are formed[41] in this stage. The last weight loss region is originating from the decomposition of nitrate species.[41] The removal of all volatile and decomposable organic components is completed at ~500 °C and a slow weight gain appears above ~600 °C due to the oxidation of nickel to form nickel oxide. From the TGA result, the calcination temperature of the gel precursor was determined

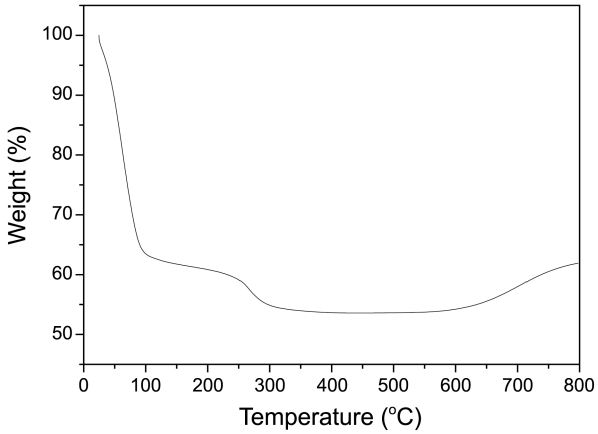

Figure 1. TGA curve of gel precursor consisting of lanthanum species with Ni powder.

to 500 °C.

Figure 2 shows the SEM and EDS data of the pristine and La-modified Ni powders after calcination at 500 °C for 3 h. From the SEM images, the Ni powder is completely covered by small particles. These La species do not cause any significant change in the size of host material, and they are well-dispersed on the surface of Ni particle. Figure 2(d) shows EDS mapping data for lanthanum of 0.50 mol % La-modified Ni powder after calcination at 500 °C. From the results of EDS, lanthanum is homogeneously distributed on Ni surface without any significant agglomeration. To investigate the structural change of the samples, XRD was measured. XRD patterns of the powder samples (not shown) obtained after calcination at 500 °C for 3 h shows only the characteristic Ni features with high intensity at 44.5, 51.9, and 76.4° (JCPDS #: 04-0850) and NiO features with low intensity at 37.2, 43.2, 62.8, 75.4, and 79.5° (JCPDS #: 47-1049) because of the partial oxidation of Ni at 500 °C. However, La-related XRD features were not observed at all

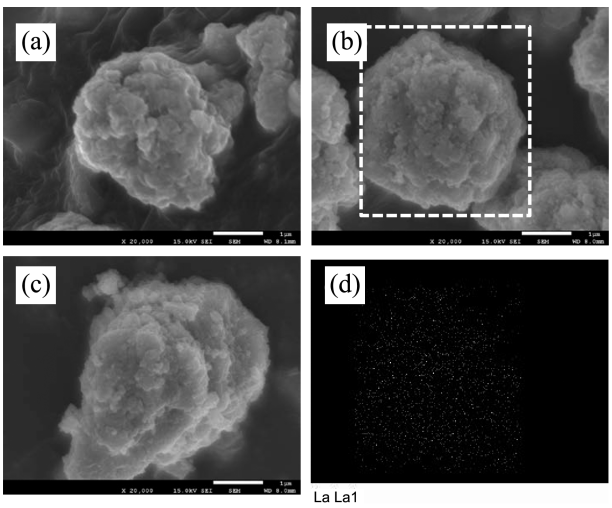

Figure 2. SEM and EDS data of the powder samples after calcination at 500 °C; (a) pristine Ni powder, (b) 0.50 mol % La-coated Ni powder, (c) 1.00 mol % La-coated Ni powder, (d) EDS data for lanthanum of (b).

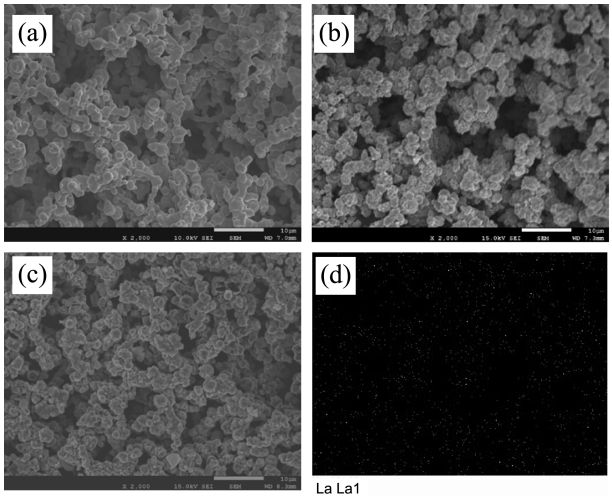

Figure 3. SEM and EDS data of the cathode after sintering under reduction condition; (a) pristine Ni cathode, (b) 0.50 mol % La-modified cathode, (c) 1.00 mol % La-modified cathode, and (d) EDS data for La of (c).

because of low concentration of lanthanum and the amorphous structure of lanthanum species.

Characterization of the Modified Cathodes. The structure of electrode is an important factor for the cell performance since the reaction occurs at ternary phase boundary among the surface of solid cathode, molten carbonate electrolyte and gas phase reactants.[42] Hence, the suitable pore size and porosity are contributed to the high performance of the MCFC. Figure 3 shows the SEM and EDS data of pristine and La-modified cathodes sintered at various temperature in the range of 750–950 °C under reduction atmosphere. The sintering temperature is different among the cathode because the modified cathode has lanthanum oxide species on the surface. The lanthanum oxide has higher melting point in comparison with Ni and NiO and the lanthanum oxide on the surface suppress the sintering between the cathode materials. This suppression causes to reduce the mechanical strength of the cathode. Therefore, the sintering temperature increases as an increase in the concentration of lanthanum species. The morphology of the modified cathode after sintering is similar to that of pristine Ni cathode as shown in Figure 3. The modified cathode also shows a good pore structure to use an MCFC cathode. Furthermore, EDS mapping images for the modified cathode material were demonstrated that lanthanum is evenly dispersed without agglomeration after tape-casting and high temperature sintering processes. The results of porosity measurement for the prepared cathodes are presented in Table 1. Even though the modified cathodes have slightly low porosity because the sintering temperature and/or sintering period are increases, their porosities are still suitable for the operation of MCFC. However, the porosity of 1.00 mol % La-modified cathode has lowest value (65.12%) because the cathode was sintered at very high temperature.

Figure 4(a) shows the XRD of the cathodes obtained after sintering in reducing atmosphere (Ar : H_2 = 70 : 30%). The

Table 1. The pore size, porosity, and bending strength data for the pristine and various La-modified cathodes

Cathode	Pore Size (μm)	Porosity (%)	Bending strength (kgf/cm^2)
Pristine Ni Cathode (sintered at 750 °C for 30 minutes)	3-7	75.20	2.73
0.10 mol % La-modified Cathode (sintered at 750 °C for 5 h)	3-7	67.27	5.27
0.50 mol % La-modified Cathode (sintered at 800 °C for 5 h)	3-7	68.25	3.61
1.00 mol % La-modified Cathode (sintered at 950 °C for 5 h)	3-7	65.12	1.33

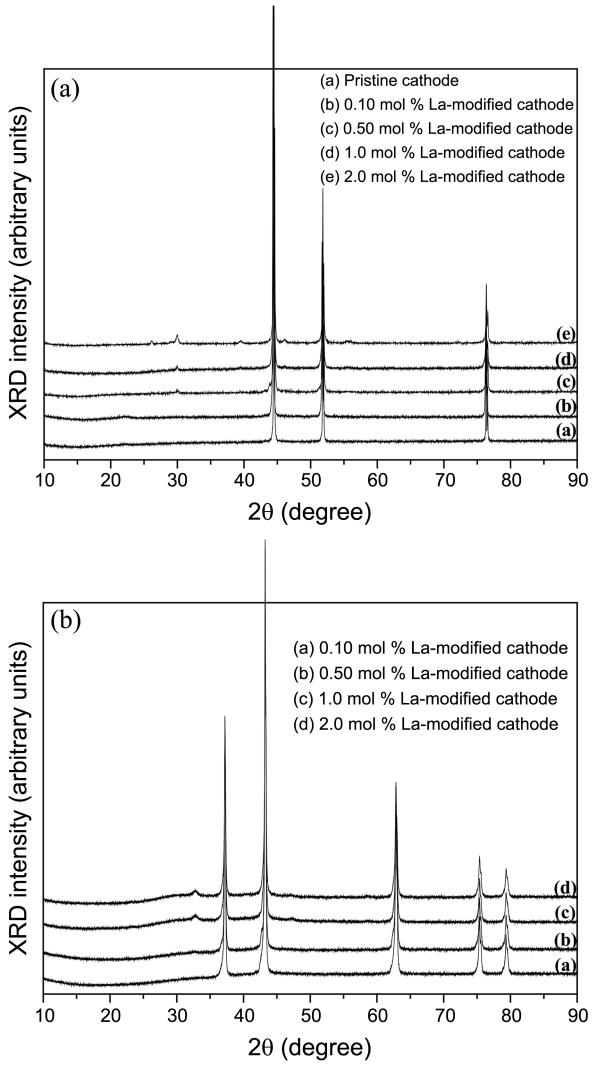

Figure 4. (a) XRD data for the pristine and the modified cathodes after sintering under the reduction conditions. (b) XRD data for the sintered cathodes after oxidation at 650 °C in the ambient atmosphere.

XRD features for NiO are completely disappeared because NiO phase formed by calcination is totally converted into metallic Ni phase due to the sintering under the reducing condition. Hence, the XRD patterns mainly show characteristic Ni scattering features (JCPDS #: 04-0805) at 44.5, 51.8, and 76.3° and some small additional features at 26.13, 29.15, 29.98, 39.56, 46.12, 52.18, and 55.49°. These additional features are assigned to La_2O_3 phase (JCPDS #: 05-0602) after sintering at high temperature. It indicates that the amorphous La species after the calcination process converts to the crystalline La_2O_3 phase and the intensity of XRD features for La_2O_3 phase systematically increases as a function of the composition of lanthanum. However, during the operation of MCFC and/or the activation of MCFC, the cathode is in the oxidizing atmosphere. Figure 4(b) shows the XRD data for the sintered cathodes after oxidation at 650 °C in the ambient atmosphere which is the similar condition as the activation of MCFC. Interestingly, XRD features of La_2O_3 completely disappear and the characteristic NiO (JCPDS #: 47-1049) at 37.2, 43.2, 62.8, 75.4, and 79.4° and other small diffraction features at 29.98, 32.77, 46.99 and 58.43° are observed. These new features are assigned to $LaNiO_3$ phase (JCPDS #: 33-0710) which is formed by the reaction of Ni and La_2O_3 at 650 °C in the ambient atmosphere. Thus-formed $LaNiO_3$ is as a typical conductive oxide having a perovskite structure and has a low electrical resistivity of ~10^{-4} Ω·cm.[43] It improves the conductivity of the electrode for the electrochemical reaction.[44] Moreover, La-modified cathode suppresses NiO dissolution and improves the mechanical strength in comparison with the pristine NiO cathode as shown in Figure 5 and Table 1. Whereas the average bending strength of pristine Ni cathode after sintering under reduction atmosphere is 1.17 kgf/cm^2,[6] that of pristine cathode oxidized at 650 °C in the ambient atmosphere is 2.73 kgf/cm^2. The bending strength of cathode, which is oxidized at 650 °C, increases in comparison with the sintered cathode because Ni converts to NiO after oxidation. The average values of 0.1 and 0.5 mol %-modified cathodes are 5.27, and 3.61 kgf/cm^2, respectively. However, due to the suppression of sintering, the cathode with high concentration of La (1.0 mol % La-modified cathode) has poor mechanical strength (1.33 kgf/cm^2) as shown in Table 1. In addition, $LaNiO_3$ phase has been reported to be formed from the

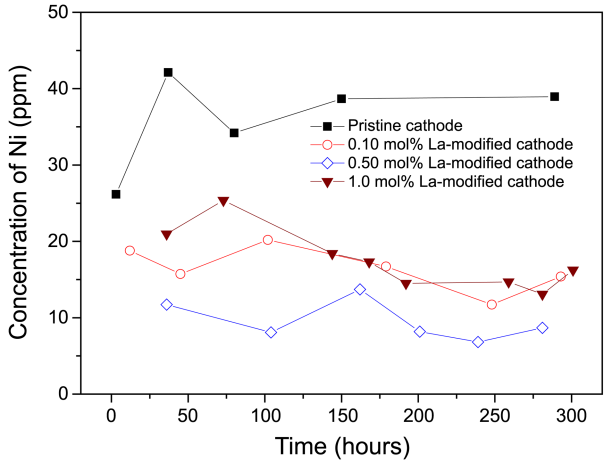

Figure 5. Solubility of pristine and La-modified cathode in molten carbobate at 650 °C for 300 h.

reaction of NiO electrode with La-saturated carbonate melts, and thus-formed $LaNiO_3$ phase significantly decreases in NiO dissolution due to the reduction of the activity of Ni in $LaNiO_3$.[16,38] The concentrations of Ni as a function of immersion time in the carbonate melts for the pristine and La-modified NiO cathodes in the molten carbonate electrolyte at 650 °C under a gas mixture of air and CO_2 (70/30%) are shown in Figure 5. The Ni concentration for pristine NiO cathode is ~38.95 ppm after 300 h. In contrast, those for La-modified NiO cathodes are significantly reduced in comparison with the pristine NiO cathode. The cathode with 0.5 mol % of La shows the lowest Ni concentration (8.678 ppm) among the samples. It is attributed to the formation of the stable protecting surface layer, $LiTiO_3$ and/or La_2O_3 [16,38] and to an increase in the basicity.[14,38,45,46]

After the solubility test, the samples were collected and investigated by XRD to figure out the degree of lithiation for cathode. Figure 6 shows XRD patterns of pristine and La-modified cathodes after solubility test at 650 °C for 300 hours. It is noted that, prior to XRD measurement, small amount of pristine Ni powder was added as an internal standard to align the XRD data. For La-modified cathodes, the XRD feature of NiO shifts to a higher angle direction in comparison with the pristine NiO cathode. The peak shift can be explained by the introduction Li^+ ions into the NiO lattice and the replacement of Ni^{2+} ions by Ni^{3+} ions causing to the decrease in the lattice parameter and the lithiated NiO has high conductivity due to the generated hole by Li dopping.[25,40,47] The lithiation process converts Ni^{2+} ions into Ni^{3+} ions which can act as positive holes and Li-doped NiO cathode has the p-type semi-conductive character.[47] Consequently, the lithated NiO and $LaNiO_3$ surface layer for the modified cathode improve the conductivity of the cathodes which can be able to enhance the cell performance.

For prospective application of MCFC in marine environments, the change of pristine and La-modified cathodes in

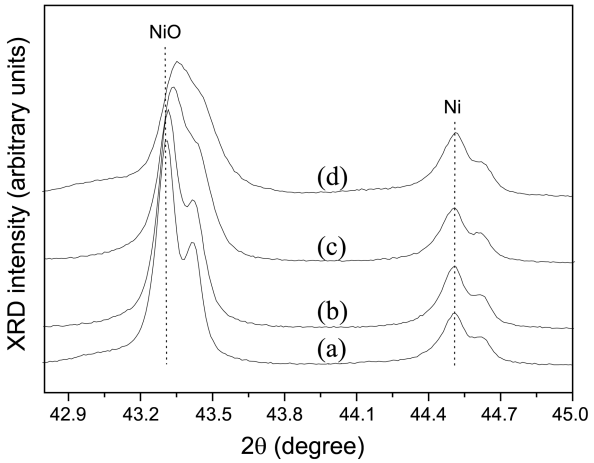

Figure 6. XRD data for the cathodes after solubility test at 650 °C for 300 h; (a) pristine cathode, (b)-(d) 0.10, 0.50, and 1.00 mol % La-modified cathodes.

10 wt % of NaCl solution, which is higher than the actual concentration of NaCl in seawater, was invetigated. In order to accelerate the corrosion reaction, the temperature of solution is set to 80 °C. As shown in Figure 7 the La-modified cathodes do not show any change of the electrode, but pristine cathode experiences the surface corrosion after 300 hours. The color change from black to green was partly observed on the pristine cathode and the green-colored chemical species were collected and investigated by IR and XRD. The XRD features were identified as a mixture of sintered cathode material and chemical species by corrosion as shown in Figure 8(a). As already mentioned, XRD patterns at 44.5, 51.9, and 76.4° (JCPDS #: 04-0850) and at 37.2, 43.2, 62.8, 75.4, and 79.5° (JCPDS #: 47-1049) are assigned to Ni and NiO of the sintered cathode, respectively. The additional X-ray diffraction features appeared at 19.3, 33.1, 38.5, 52.1, 59.1, and 62.7° are consistent with nickel hydroxide

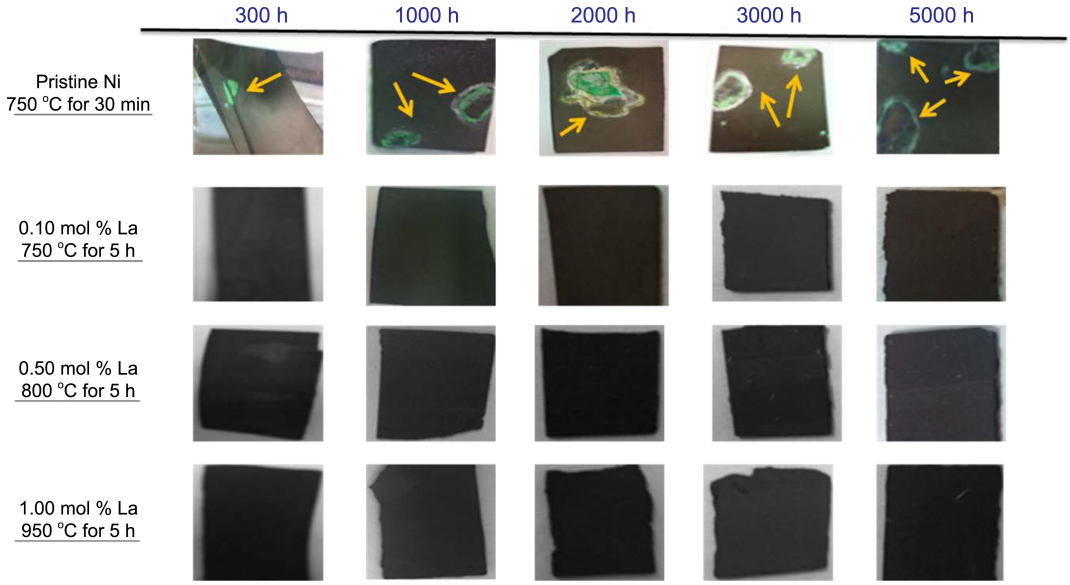

Figure 7. Images of pristine Ni and La-modified Ni cathode after immersion in 10 wt % NaCl solution as a function of immersion times.

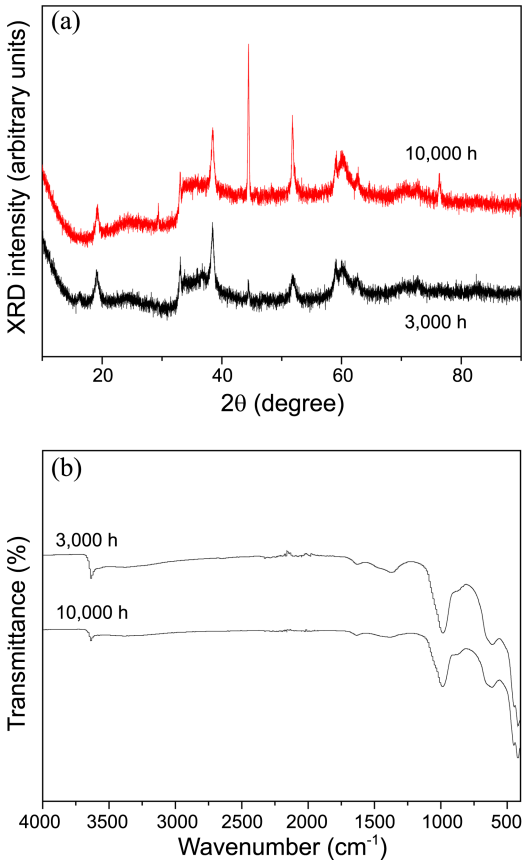

Figure 8. (a) XRD and (b) IR data of the chemical species by corrosion of pristine Ni cathode after immersion in 10 wt % NaCl solution.

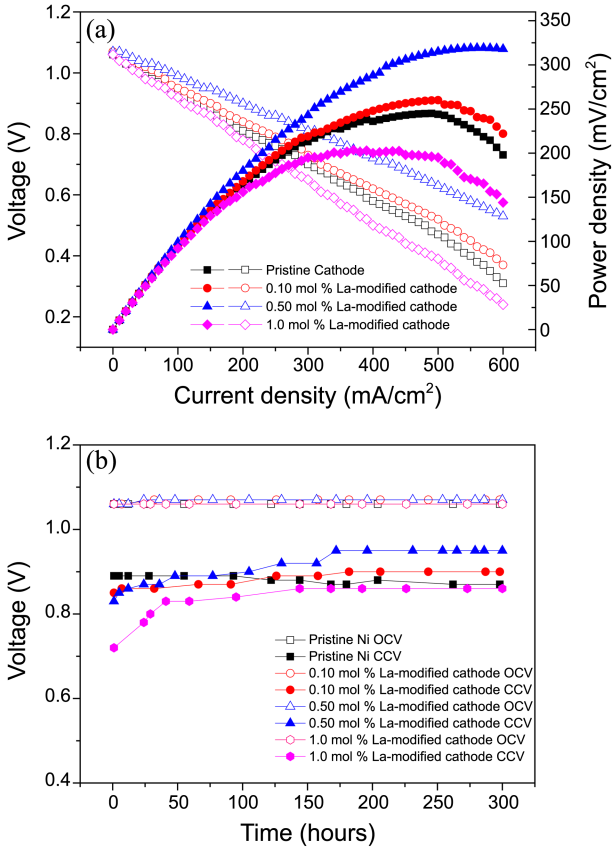

Figure 9. (a) Voltages and power densities as a function of current density. (b) The results for longevity (OCV and CCV) at the current density of 150 mA/cm^2.

(JCPDS #: 14-0117). To further support the XRD data, FT-IR spectroscopy was performed with the collected sample and the spectra are shown in Figure 8(b). The peaks at 3640 cm^{-1} and the band near 520 cm^{-1} are attributed to the OH stretching and OH bending vibrations, respectively. The peaks at 620 and 480 cm^{-1} are associated with the Ni–OH bending and Ni–O stretching vibrations, respectively.

Unit Cell Performance. Figure 9(a) and (b) show voltage and power density as a function of current density and longevity test results for the pristine and La-modified NiO cathodes, respectively. The open-circuit voltage (OCV) and closed-circuit voltage (CCV) of MCFC with the pristine NiO cathode are 1.06 and 0.87 V at the current density of 150 mA/cm^2, respectively. Whereas, OCV and CCV of the cell with 0.5 mol % La-modified cathode are 1.07 and 0.95 V at the same current density, respectively. The La-modified NiO cathode has higher power and more stable performance in comparison with pristine NiO cathode. However, the differences of voltages and power densities between pristine and La-modified NiO cathodes are more significant as the current density increases. The slope of the voltage for the pristine NiO at ~500 mA/cm^2 starts to decrease and, as a result, the power density has the maximum value. The further increase in the current density shows the reduction of power density. When current is flow, the voltage have a value lower than the theoretical OCV due to electrode reactions and the occurrence of overvoltage contain polarization as activation polarization (charge transfer loss), ohmic polarization and concentration polarization (mass transfer loss). The slope of the voltage at ~500 mA/cm^2 is sharply decreases to limiting current density. As flow of high current density, the concentration polarization becomes large due to reaction material for electrode is slow supply. However, the power density for 0.5 mol % La-modified cathode shows the gradual increase upto at least 600 mA/cm^2. The high performance of La-modified cathode is attributed to the enhanced conductivity[43,44,48] and catalytic activity[26,35,39] of $LaNiO_3$ surface layer. Moreover, L. Daza *et al.* observed that the La improve charge transfer processes associated with the oxygen reduction, and La-incorporation of Ni cathode showed impedance values lower than pristine Ni cathode due to their higher conductivities.[22,23] Therefore, these cathodes reduce the ohmic loss causing an improvement of the cell performance. Furthermore, the degree of lithiation of the modified cathode measured by XRD is increased in comparison with the pristine NiO cathode as shown in Figure 6. The NiO cathode is transformed into lithiated NiO ($Li_xNi_{1-x}O$), and the the conductivity of NiO is increased by generated hole as Li. Even though the amount of La in the modified NiO cathode increase the degree of lithiation, the modified NiO cathode with high concentration of La shows a poor cell performance because it has a poor porosity due to the high sintering

temperature.

Conclusion

The La-modified Ni powders as a new cathode material of MCFC have been successfully prepared using a polymeric precursor based on the Pechini method. The morphology of the La-modified Ni cathode after sintering is similar to that of the pristine Ni cathode and it shows good pore structure and mechanical strength for MCFC cathode. In addition, the modified cathode does not show the morphological change and physical/chemical effect at marine environment. The La-modified cathode material has $LaNiO_3$ phase after sintering and oxidation process and this $LaNiO_3$ phase has high conductivity and resistivity for the corrosion in molten carbonate mixture. Furthermore, La-modified cathode shows higher degree of lithiation in molten catbonate and lower NiO dissolution in comparison with pristine cathode. Due to these positive effects, the cell performance and the longevity of the cell are dramatically improved. The results obtained in this study are demonstrated that La-modified NiO cathode has high cell performance. Specifically, La-modified NiO cathode is more stable and more powerful because of the formation of $LaNiO_3$, high degree of lithiation, and low dissolution of NiO.

Acknowledgments. This work was supported by the New & Renewable Energy of the Korea Institute of Energy Technology Evaluation and Planning (KETEP) grant funded by the Korea government Ministry of Knowledge Economy.

References

1. Spiegel, C. *Designing and Building Fuel Cells*; Mcgraw-hill: 2007.
2. Song, S. A.; Kim, H. K.; Ham, H. C.; Han, J.; Nam, S. W.; Yoon, S. P. *J. Power Sources* **2013**, *232*, 17.
3. Yi, C.-W.; Kwak, J. H.; Peden, C. H. F.; Wang, C.; Szanyi, J. *J. Phys. Chem. C* **2007**, *111*, 14942.
4. Alkaner, S.; Zhou, P. L. *J. Power Sources* **2006**, *158*, 188.
5. Huber, C.; Klimant, I.; Krause, C.; Werner, T.; Mayr, T.; Wolfbeis, O. S. *Fresen. J. Anal. Chem.* **2000**, *368*, 196.
6. Ganesan, P.; Colon, H.; Haran, B.; White, R.; Popov, B. N. *J. Power Sources* **2002**, *111*, 109.
7. Ito, Y.; Tsuru, K.; Oishi, A.; Miyazaki, Y.; Kodama, T. *J. Power Sources* **1988**, *23*, 357.
8. Baumgartner, C. E. *J. Am. Ceram. Soc.* **1986**, *69*, 162.
9. Ota, K.; Mitsushima, S.; Kato, S.; Asano, S.; Yoshitake, H.; Kamiya, N. *J. Electrochem. Soc.* **1992**, *139*, 667.
10. Morita, H.; Komoda, M.; Mugikura, Y.; Izaki, Y.; Watanabe, T.; Masuda, Y.; Matsuyama, T. *J. Power Sources* **2002**, *112*, 509.
11. Desilvestro, J.; Haas, O. *J. Electrochem. Soc.* **1990**, *137*, C5.
12. Scott, K.; Kang, M. P.; Winnick, J. *J. Electrochem. Soc.* **1983**, *130*, 527.
13. Choi, H. J.; Ihm, S. K.; Lim, T. H.; Hong, S. A. *J. Power Sources* **1996**, *61*, 239.
14. Doyon, J. D.; Gilbert, T.; Davies, G.; Paetsch, L. *J. Electrochem. Soc.* **1987**, *134*, 3035.
15. Matsuzawa, K.; Akinaga, Y.; Mitsushima, S.; Ota, K. *J. Power Sources* **2011**, *196*, 5007.
16. Matsuzawa, K.; Mizusaki, T.; Mitsushima, S.; Kamiya, N.; Ota, K. *J. Power Sources* **2005**, *140*, 258.
17. Matsuzawa, K.; Tatezawa, G.; Matsuda, Y.; Mitsushima, S.; Kamiya, N.; Ota, K. *J. Electrochem. Soc.* **2005**, *152*, A1116.
18. Mitsushima, S.; Matsuzawa, K.; Kamiya, N.; Ota, K. *Electrochim. Acta* **2002**, *47*, 3823.
19. Ota, K. I.; Matsuda, Y.; Matsuzawa, K.; Mitsushima, S.; Kamiya, N. *J. Power Sources* **2006**, *160*, 811.
20. Tanimoto, K.; Miyazaki, Y.; Yanagida, M.; Kojima, T.; Ohtori, N.; Kodama, T. *Denki Kagaku* **1995**, *63*, 316.
21. Tanimoto, K.; Miyazaki, Y.; Yanagida, M.; Tanase, S.; Kojima, T.; Ohtori, N.; Okuyama, H.; Kodama, T. *J. Power Sources* **1992**, *39*, 285.
22. Escudero, M. J.; Novoa, X. R.; Rodrigo, T.; Daza, L. *J. Power Sources* **2002**, *106*, 196.
23. Escudero, M. J.; Rodrigo, T.; Daza, L. *Catal. Today* **2005**, *107-08*, 377.
24. Hong, M. Z.; Bae, S. C.; Lee, H. S.; Lee, H. C.; Kim, Y. M.; Kim, K. *Electrochim. Acta* **2003**, *48*, 4213.
25. Hong, M. Z.; Lee, H. S.; Kim, M. H.; Park, E. J.; Ha, H. W.; Kim, K. *J. Power Sources* **2006**, *156*, 158.
26. Huang, B.; Chen, G.; Li, F.; Yu, Q. C.; Hu, K. A. *Electrochim. Acta* **2004**, *49*, 5055.
27. Kim, M. H.; Hong, M. Z.; Kim, Y. S.; Park, E.; Lee, H.; Ha, H. W.; Kim, K. *Electrochim. Acta* **2006**, *51*, 6145.
28. Kuk, S. T.; Song, Y. S.; Suh, S.; Kim, J. Y.; Kim, K. *J. Mater. Chem.* **2001**, *11*, 630.
29. Okawa, H.; Lee, J. H.; Hotta, T.; Ohara, S.; Takahashi, S.; Shibahashi, T.; Yamamasu, Y. *J. Power Sources* **2004**, *131*, 251.
30. Park, E.; Hong, M. Z.; Lee, H.; Kim, M.; Kim, K. *J. Power Sources* **2005**, *143*, 84.
31. Baumgartner, C. E.; Arendt, R. H.; Iacovangelo, C. D.; Karas, B. R. *J. Electrochem. Soc.* **1984**, *131*, 2217.
32. Bockris, J. O.; Otagawa, T. *J. Electrochem. Soc.* **1984**, *131*, 290.
33. Franke, M.; Winnick, J. *J. Electrochem. Soc.* **1988**, *135*, 1595.
34. Ganesan, P.; Colon, H.; Haran, B.; Popov, B. N. *J. Power Sources* **2003**, *115*, 12.
35. Huang, B.; Wang, S. R.; Yu, Q. C.; Liu, Y.; Hu, K. A. *J. Appl. Electrochem.* **2005**, *35*, 1145.
36. Plomp, L.; Veldhuis, J. B. J.; Sitters, E. F.; Vandermolen, S. B. *J. Power Sources* **1992**, *39*, 369.
37. Suntivich, J.; Gasteiger, H. A.; Yabuuchi, N.; Nakanishi, H.; Goodenough, J. B.; Shao-Horn, Y. *Nat. Chem.* **2011**, *3*, 546.
38. Scaccia, S.; Frangini, S.; Dellepiane, S. *J. Mol. Liq.* **2008**, *138*, 107.
39. Kim, Y.-S.; Yi, C.-W.; Choi, H. S.; Kim, K. *J. Power Sources* **2011**, *196*, 1886.
40. Mekhemer, G. A. H.; Balboul, B. A. A. *Colloids Surf. A* **2001**, *181*, 19.
41. Escudero, M. J.; Rodrigo, T.; Mendoza, L.; Cassir, M.; Daza, L. *J. Power Sources* **2005**, *140*, 81.
42. Hwang, D. K.; Kim, S.; Lee, J.-H.; Hwang, I.-S.; Kim, I.-D. *J. Mater. Chem.* **2011**, *21*, 1959.
43. Liang, K.; Wang, N.; Zhou, M.; Cao, Z.; Gu, T.; Zhang, Q.; Tang, X.; Hu, W.; Wei, B. *J. Mater. Chem. A* **2013**, *1*, 9730.
44. Matsuzawa, K.; Akinaga, Y.; Mitsushima, S.; Ota, K.-i. *J. Power Sources* **2011**, *196*, 5007.
45. Matsuzawa, K.; Mizusaki, T.; Mitsushima, S.; Kamiya, N.; Ota, K.-i. *J. Power Sources* **2005**, *140*, 258.
46. Mitsushima, S.; Matsuzawa, K.; Kamiya, N.; Ota, K.-i. *Electrochim. Acta* **2002**, *47*, 3823.
47. Daza, L.; Rangel, C. M.; Baranda, J.; Casais, M. T.; Martinez, M. J.; Alonso, J. A. *J. Power Sources* **2000**, *86*, 329.
48. Miyake, S.; Fujihara, S.; Kimura, T. *J. Eur. Ceram. Soc.* **2001**, *21*, 1525.